Journal of Colloid and Interface Science 614 (2022) 451–459

Contents lists available at ScienceDirect

Journal of Colloid and Interface Science

journal homepage: www.elsevier.com/locate/jcis

Environmentally friendly ZnO/Castor oil polyurethane composites for the gas-phase adsorption of acetic acid

Alessio Zuliani, Damiano Bandelli, David Chelazzi, Rodorico Giorgi, Piero Baglioni *

Department of Chemistry "Ugo Schiff" and CSGI, University of Florence, Via della Lastruccia 3, Sesto Fiorentino, Florence 50019, Italy

GRAPHICAL ABSTRACT

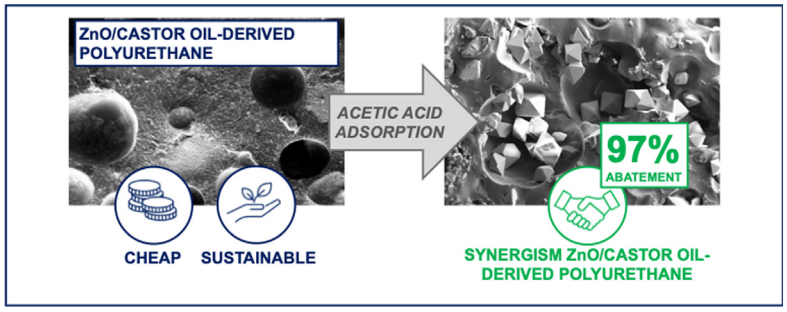

ARTICLE INFO

Article history:
Received 10 December 2021
Revised 18 January 2022
Accepted 19 January 2022
Available online 24 January 2022

Keywords:
Art conservation
Polyurethanes
Castor oil
Acetic acid
VOCs
Zinc oxide

ABSTRACT

Hypothesis: Acetic acid, a common pollutant present in museums and art galleries, can irreversibly damage works of art. Herein, a sustainable and scalable synthesis of zinc oxide-castor oil polyurethane hybrids (ZnO/COPs), to be used as acetic acid removers in the preventive conservation of Cultural Heritage, is reported.

Experiments: The adsorption capacities of ZnO/COPs were studied in saturated acetic acid atmosphere, at low acetic acid gas concentration, and inside a wooden crate (naturally emitting acetic acid) representative of those used in the storage deposits of museums and art collections.

Findings: Upon exposure, acetic acid interacts with the castor oil polyurethane and diffuses to the surface of ZnO particles where is stably fixed as zinc acetate crystals. Zinc acetate domains form homogeneously on the surface and are distributed evenly within the ZnO/COPs, thanks to weak interactions between the polyurethane matrix and acetic acid that favour the transport of the acid up to reach the zinc oxide surfaces, resulting in a synergistic effect. The ZnO/COPs composites showed significantly enhanced adsorption capacities of acetic acid surpassing those of the activated carbon benchmark, with the advantage of being easily handled and movable, without the health issues and risks associated to the use of non-confined micro/nano-powders.

1. Introduction

The purification of air from volatile organic compounds (VOCs) [1] prevents and limits the degradation of works of art and historical objects exposed or stored in museums, collections, and art galleries.[2,3] Indeed, VOCs can damage sensitive materials and irreversibly change the appearance and structural properties of artifacts. In particular, acetic acid (AcOH), which mostly derives from the degradation of cellulosic materials (*i.e.*, books, frames, wooden boxes, *etc.*) and restoration adhesives,[4] is one of the most abundant VOCs present in museums and art galleries, and one of

* Corresponding author.
E-mail address: piero.baglioni@unifi.it (P. Baglioni).

https://doi.org/10.1016/j.jcis.2022.01.123
0021-9797/

the most corrosive.[5–7] For example, alkyd resin, a commonly used binder for paints, shows rapid degradation when exposed to AcOH vapors, resulting in the formation of a white patina on the surface of the paintings.[8] In addition, some historical inorganic pigments (*e.g.*, azurite, white lead, red lead and lead–tin yellow) tend to form new crystalline phases when exposed to AcOH vapors, lightening or darkening the paint colours.[9] For example, magnificent skies in Raffaello's "The Miraculous Draft of Fishes" or in Rubens' "Autumn Landscape with a View of Het Steen in the Early Morning", were painted with azurite and would be dramatically altered if exposed to this VOC. Thus, the removal of AcOH in art galleries, museums and storage deposits is crucial for the preventive conservation of our artistic and historical heritage.

Different materials are employed as efficient VOCs removers, ranging from activated carbons to zeolites, metal–organic frameworks (MOFs), and hypercrosslinked polymeric resins (HPR). The VOCs removal properties of these materials vary greatly, *e.g.*, zeolites have an average adsorption capacity (reported as mg of VOCs *per* gram of adsorbing material) of 460 mg g^{-1}; activated carbons of 140 mg g^{-1}; HPR of 380 mg g^{-1}, and MOFs of 800 mg g^{-1}.[10] However, while the development of most state-of-the-art removers has so far focused on boosting adsorption properties, other crucial factors have been overlooked, such as manufacturing costs, the use of sustainable materials, and the overall up-scalability of the production process. These have become critical aspects that must be addressed to preserve, in a sustainable way, large collections worldwide where thousands of objects are exposed and stored, as an example MOMA (USA) has about 200,000 and Centre Pompidou (France) more than 100,000 artifacts to be preserved. For instance, MOFs are highly promising in terms of VOCs adsorption, but their manufacturing costs considerably limit their use.[11] Synthetic zeolites, such as SBA-15 or MCM-41, are employed as catalysts in the chemical industry, and they can be quickly reactivated and recycled, amortizing their costs over many production cycles.[12–14] However, if considered as VOCs removers in art collections, and in particular inside crates in storage deposit, their utilization should last for years, and their usage would be too expensive even considering recycling. Activated carbons, natural porous materials and natural zeolites represent good compromises between low manufacturing costs and environmentally friendly characteristics.[15–18] Activated carbons are cost-effective thanks to their biomass nature, since they can be produced from coconut shells, walnuts shells, woods, and other sources.[19,20] Natural porous materials such as diatomite, stellerite, and vitric tuff have low environmental impact and could be used as VOCs remover after some easy feasible activation steps.[21] Nevertheless, all these absorbers come as micro/nano-powders, requiring the use of filters, since they can be dispersed in air or on surfaces during handling, potentially affecting the artworks, or causing health issues.[22,23] Most importantly, these powders mainly adsorb VOCs *via* physisorption, and can release them in a large amounts when atmospheric conditions change (*e.g.*, due to temperature fluctuations), actually turning into sources of VOCs.[24,25]

Finally, hypercrosslinked polymeric resins are relatively inexpensive and have good VOCs adsorption capacities; however, they are typically petroleum-based, and thus their use should be carefully evaluated according to sustainable environmental policies.[26–31]

Overall, the development of reliable (non-powdery) VOCs adsorption materials with low environmental impact, low production costs, and high adsorption capacities, is still an open challenge.

In the present work, a novel environmentally friendly hybrid (organic–inorganic) hypercrosslinked resin for the removal of AcOH, composed of zinc oxide supported and incorporated into a polyurethane structure derived from castor oil, is described. A biomass-derived hypercrosslinked polyurethane of castor oil and poly(hexamethylene diisocyanate) was used as sustainable polymer, while ZnO, opportunely confined in the matrix, was employed as safe and almost non toxic AcOH remover, taking advantage of the formation of zinc acetate. *To the best of our knowledge, no such approach has been reported yet for the design of environmentally friendly, compact organo-inorganic systems for the efficient removal of VOCs and in particular AcOH.* A series of ZnO-castor oil polyurethane composite systems (ZnO/COPs) was prepared using three types of ZnO powders, with particles size distributions ranging from 20 nm to 44 μm and different commercial availabilities. The exploitation of the high surface area to volume ratios of zinc oxide nanoparticles specifically aimed at increasing the overall performances of the ZnO/COPs.[32–34] The adsorption capacities of ZnO/COPs hybrids were studied in different types of AcOH atmosphere, and the novel composites were fully characterized by infrared spectroscopy, thermogravimetric analysis, and scanning electron microscopy, before and after the adsorption tests. The high adsorption capacities of the novel composites and their ability to retain AcOH were related to the diffusion of AcOH through the COP matrix up to reach ZnO particles, which was investigated mapping the formation of zinc acetate by 2D infrared imaging. Besides, the color change of the ZnO/COPs hybrids was monitored after exposition to AcOH, which could be possibly exploited in practical applications to determine the saturation limit of the composites and the need of their replacement.

2. Materials and methods

2.1. Materials

Castor oil (Pharma grade, 89.2%$_{wt}$ of ricinoleic acid) was purchased from Gioma Varo Srl (Milan, Italy). Poly(hexamethylene diisocyanate) (polyHDI, 1,300–2,200 cP), ZnO powder (<5 μm particle size, 99.7% calculated on calcined substance), ethanol (absolute, reag. ISO, reag. Ph. Eur., ≥99.8% (GC)), and acetic acid (glacial, ReagentPlus®, ≥99%) were purchased form Sigma Aldrich (Milan, Italy). ZnO nanopowder (average particles size 20 nm, >99% trace metals basis) was purchased from Ionic Liquids Technologies GmbH (Heilbronn, Germany). Commercially available (for industrial purposes) ZnO powder (particle size < 44 μm, >99.9%, Pharama grade "Gold") was purchased from L'Aprochimidie Srl (Muggiò, Italy). Activated charcoal (Activated Charcoal K48, from coconut shells) was purchased from Long Life for Art GmbH (Eichstetten, Germany). All reagents were used without any further purification. ZnO powders were dried at 393 K during 48 h before utilization, to remove all eventually adsorbed moisture.

2.2. Synthesis of the ZnO/COPs composites

The ZnO/COPs were prepared by modifying and upgrading a reported procedure for the preparation of cross-linked castor oil-based adhesives.[35–37] In details, castor oil and poly(hexamethylene)diisocyanate (PolyHDI) were firstly vigorously stirred for 15′. Then, ZnO powders (10, 30 or 60%$_{wt}$) were added and mixed for other 15′. Finally, the mixture was poured into silicone molds and cured in oven (343–373 K). After the curing step, ZnO/COPs were removed from the molds and used for characterization analyses, as well as for VOCs adsorption tests, without any further modification.

2.3. Characterization techniques of the ZnO/COPs composites

Thermogravimetric analyses were carried out with an SDT Q600 analyzer (TA Instrument Inc., USA) operating with aluminum pans. The samples were heated from 298 up to 850 K at 10 K min^{-1} in

nitrogen atmosphere (100 mL·min^{-1}). Prior to analysis, the materials were conditioned at 298 K under nitrogen flux (100 mL·min^{-1}) for 10 min. The analyses were performed under a nitrogen flux of 100 mL·min^{-1} for both the balance and the sample. SEM images were recorded with a FEG-SEM Gemini scanning microscope (Carl Zeiss Microscopy, Germany), working at 5–15 kV and a 3.7 – 4.4 mm working distance.

Attenuated total reflection Fourier Transformation Infrared spectroscopy (FTIR-ATR) measurements were carried out with a Thermo Nicolet Nexus 870 spectrometer equipped with a liquid nitrogen-cooled MCT detector and a single reflection diamond crystal ATR unit. The analyses were performed in an absorbance mode, using a spectral resolution of 4 cm^{-1}, and acquiring 32 scans for each spectrum in the spectral range from 4000 to 650 cm^{-1}.

2D FTIR imaging was performed with a Cary 670 FTIR spectrophotometer coupled to a Cary 620 FTIR microscope (Agilent Technologies), using a 15x Cassegrain objective. Measurements were carried out in reflectance mode over a gold-plated reflective surface; background spectra were collected directly on the gold-plated surface. The FTIR settings were as follows: 128 scans for each acquisition, spectral resolution of 8 cm^{-1}, open windows, and spectral range of 3900–900 cm^{-1}. A 128 × 128 pixels Focal Plane Array (FPA) detector was used, where each pixel has dimensions of 5.5 μm × 5.5 μm^2 and produces an independent spectrum.

XRD patterns were recorded with a Bruker D8 Advance diffractometer (Bruker Corporation, Billerica, USA) with CuKα (λ = 1.54 18 Å) radiation. Wide angle scanning patterns were collected over a 2θ range from 10° to 80° with a step size of 0.018° and counting time of 2 s per step.

Color changes of the ZnO/COPs after adsorption tests in saturated atmosphere of AcOH, were investigated by collecting macro photographs with a professional camera (Canon EOS 60D 18 MP camera equipped with a Canon EF-S 17–85 mm f/4–5.6 USM SLR lens).

2.4. VOCs adsorption tests

The adsorption capacities of the ZnO/COPs were firstly determined by gravimetric analysis using sealed microchambers with saturated atmosphere of AcOH.[38] In each experiment, a cylinder of ZnO/COP (4 g, 36 mm diameter, 4 mm height) and a 10 mL vial filled with 8 mL AcOH were closed and sealed in a 120 mL glass sample container equipped with a screw cap, and placed in a thermal chamber at 295.0 ± 1.5 K. Each ZnO/COP cylinder was regularly weighted, stopping when a stable value (<5% difference with the previous measurement) was observed for at least 100 h. Similarly, 4 g of pure ZnO powders or activated charcoal (used as benchmark), were placed in 10 mL vials, and their adsorption capacities were studied in the same way as for the ZnO/COPs cylinders. After more than 1500 h of adsorption, equilibrium was reached, and adsorption capacities were calculated as the ratio between the adsorbed acetic acid (mg) and the initial mass of the material. [39] After adsorption tests in saturated atmosphere of AcOH, the samples were placed in a drying chamber under vacuum (15 mbar). Samples were regularly weighted until a stable value (<2% difference with the previous measurement) was measured for at least 48 h.

Adsorption tests at low initial concentration of AcOH (in the order of ppmv – volumetric part *per* million) were carried out by placing the samples inside 54 L glass single neck flat bottom flasks filled with 25 μL of 1M AcOH solution, and the atmosphere was analyzed according to the analytical method OSHA PV2119 [40] (see Supplementary Material section S1 for details).

Finally, to simulate the real case scenario of storage deposits in museums and collections, adsorption tests were also performed in a 630 L wooden crate (1.0 × 0.9 × 0.7 m) naturally emitting AcOH. [41] ZnO/COPs were prepared in the form of eight rectangular strips of 40 × 80 × 5 mm, each weighting 12.5 g. The AcOH content inside the wooden crate was measured before and after the addition of the ZnO/COPs (according to OSHA PV2119). The experiment was run for 45 days, measuring the AcOH concentration weekly.

3. Results and discussion

The ZnO/COPs were synthesized by modifying and upgrading a process previously reported for the preparation of cross-linked castor-oil based adhesives, as schematically illustrated in Fig. 1. [36]

The building of the polyurethane network took place through the nucleophilic attack of the hydroxyl groups of ricinoleic acid, the main component of castor oil (present in the form of triglycerides composed by one, two or three ricinoleic acid chains, and oleic/linoleic acid chains), onto different types of (poly) diisocyanate groups.[42–45] The reported synthesis[36] produced castor oil-polyurethanes resins whose flexibility and stickiness depended on the amount of unreacted castor oil incorporated in the polyurethane network, which in that case was regulated to control the adhesive properties of COPs. For the purpose of the present work, the presence of free hydroxyl groups in unreacted oil was deemed an important feature, as they were expected to interact with AcOH. Thus, preliminary steps aimed at optimizing the adsorption properties of COPs prior to the addition of ZnO. PolyHDI, rather than its monomer form, was selected to react with castor oil, due to its low volatility (<0.00003 hPa vapor pressure at 293 K) that made its use safer than HDI and other isocyanates such as methylene diphenyl diisocyanate (MDI) or toluene diisocyanate (TDI). COPs were then synthesized minimizing the amount of employed PolyHDI (which is derived from petroleum) to maximize the amount of free hydroxyl groups in the network and increase the overall sustainability and affordability of the process. Two important synthetic parameters were varied, *i.e.*, the curing temperature (343–373 K) and time (3–48 h), by monitoring the castor oil-PolyHDI polymerization competition (*i.e.*, the disappearing of the isocyanate peak at 2274 cm^{-1} in the ATR-FTIR spectra of the COPs, see also section S2 in the Supplementary Material)[46] and investigating the adsorption capacities of the so-produced materials. The initial castor oil:PolyHDI ratio of 82:18 (%$_{wt}$) was selected according to the literature.[35,36] Overall, the best curing parameters were found to be 363 K for 24 h, as a balance between high absorption capacity and low energy consumption. Several castor oil:PolyHDI ratios were studied, finally selecting 83:17 (%$_{wt}$) (corresponding to an approximatively NCO/OH ratio of *ca.* 0.4) as an optimal compromise between raw materials costs, adsorption capacities and handling properties of the COPs (the lower the amount of PolyHDI, the stickier the material, due to higher amount of free hydroxyl groups of unreacted castor oil on the surface). The relative amount (%) of unreacted hydroxyls in the COPs was estimated to be *ca.* 85%, which was calculated considering one mole of –OH per mole of ricinoleic acid (89.2%$_{wt}$ in castor oil), and then subtracting the isocyanate moles, considering a 1:1 stoichiometry for the hydroxyl-isocyanate reaction, a ∼ 23%$_{wt}$ isocyanate content in PolyHDI (according to the producers), and a complete isocyanate reaction (as *per* ATR-FTIR measurements, see above and section S2 of the Supplementary Material).

The optimized COP synthesis was then used to prepare a series of ZnO/COPs, varying the ZnO content up to 60%$_{wt}$ and employing ZnO powders with different particles size. The incorporation of more than 60%$_{wt}$ ZnO made the COPs crumbling. Table 1 lists the ZnO/COPs formulations selected for investigation in the present work, along with the ZnO powders references used.

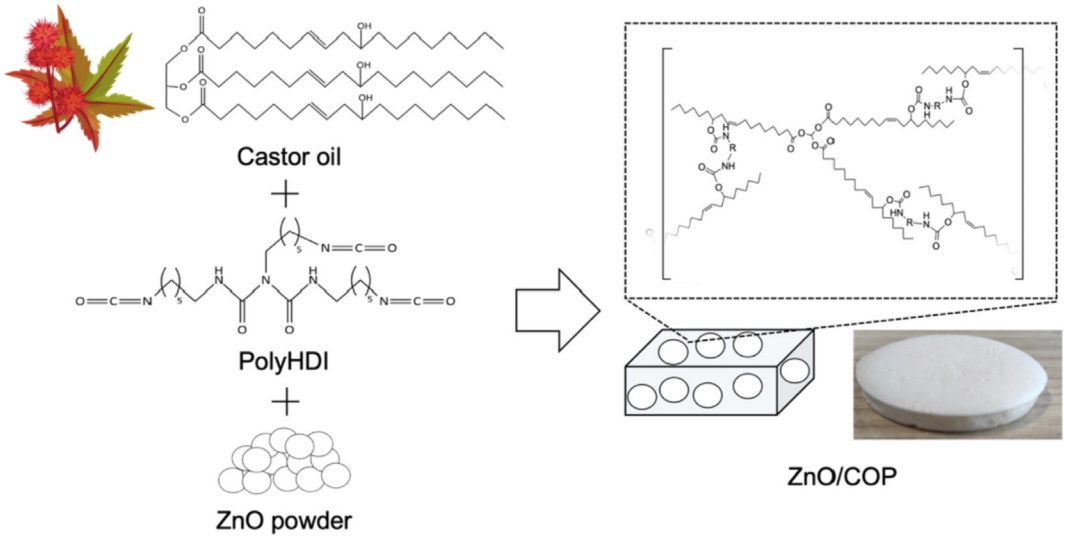

Fig. 1. Scheme of the preparation of ZnO/COPs.

Table 1
ZnO/COPs samples synthesized at 363 K, using a castor oil:PolyHDI ratio of 83:17 (%).

Sample name	Type of ZnO	ZnO $\%_{wt}$	Reaction parameters
COP	/	0	83:17 ($\%_{wt}$) castor oil:
10n	20 nm average particles size	10	PolyHDI, 363 K
30n		30	
60n		60	
10e	EMPROVE® E. < 5 μm	10	
30e	particle size	30	
60e		60	
10g	<44 μm, particles for	10	
30g	industrial purposes	30	
60g		60	
ZnO-n	20 nm average particles size	100	Used as pure powders
ZnO-e	EMPROVE® E, <5 μm	100	
ZnO-g	<44 μm, particles for industrial purposes	100	

The scalability and sustainability of the synthesis of ZnO/COPs were evaluated through the determination of some green metrics, specifically Reaction Mass Efficiency (RME) and Environmental factor (E-factor).[47,48] The value of RME (% of the ratio of the mass of the desired product divided by the sum of the masses of all the reagents) was ~ 100%, thanks to the complete reaction of castor oil with PolyHDI, and owing to the complete incorporation of ZnO in the polyurethane network with no detectable losses.

Because the reaction was solvent free, the only waste derived from the use of a solution (50:50 ($\%_{wt}$) water:ethanol) for washing the molds and the reactor. Accordingly, an E-Factor of 0.3 was calculated for the process (*i.e.*, the ratio of the total mass of waste (kg) divided by the total mass of the product (kg)).[49] Such a low value positioned the synthetic procedure in the bulk chemicals industrial sector, close to oil refining, and remarkably below the fine chemical and the pharmaceutical sectors.[50] Moreover the *ZnO/COPs are made from castor oil, derived from the nonedible beans of the castor plant (ricinus communis), a natural and renewable resource whose crops have no ethical impact on human nutrition.*[51,52] Finally, zinc oxide, a non-toxic material, largely used in cosmetics, could be also produced from zinc-containing waste, with no impact on zinc reserves (*i.e.*, ores).[53–55] These characteristics, in addition to the simplicity of the process, classify the synthesis of ZnO/COPs as easily up-scalable, sustainable, and environmentally friendly.

ZnO/COPs composites were produced as white flexible materials, where zinc oxide particles are distributed homogeneously through the section and in the pores of the polyurethane network, as shown by SEM images in Fig. 2 (see section S3 in the Supplementary Material for additional images).

The COPs exhibited a compact morphology, both at the surface (Fig. 2, A) and through their section (Fig. 2, B). Instead, when ZnO was embedded in the polyurethane, bubble-like cavities of 10–350 μm were formed in the network (Fig. 2, D, F, H and L), likely owing to gaseous CO_2 produced by the reaction of isocyanate with water (dissolved in castor oil). According to the data provided by the supplier, and as confirmed by TGA and DTG analyses (see section S4 in the Supplementary Material), castor oil has moisture content of approximately 0.1 $\%_{wt}$. The reaction was favored by the presence of ZnO that acted as catalyst for the nucleophilic attack of hydroxyl groups to isocyanate.

As illustrated in Fig. 3 A, the TGA and DTG curves of pure castor oil showed three degradation steps. According to the literature, the first step, between 550 and 680 K, corresponds to the decomposition and/or volatilization of highly volatile and unstable compounds such as oxygenated compounds, hydroperoxides, and poly unsaturated fatty acids; the second step, in the 680–720 K range, corresponds to the degradation of monosaturated fatty acids, while the third step, ranging from 720 to 760 K, corresponds to the decomposition of saturated fatty acids.[56,57] These degradation steps were also observed in the TGA and DTG curves of COPs, with an additional degradation step between 530 and 630 K, ascribed to the degradation of urethane linkages. When ZnO was added, the thermal decompositions of both pure castor oil and COP were catalyzed, as shown in Fig. 3 B ("castor oil + ZnO" relates to the TGA and DTG curve of a 50:50 (w/w) mixture of castor oil and ZnO powder), where the degradation of castor oil and urethane linkages are observed at lower temperatures or as peak shoulders.

Even though ZnO catalyzed the thermal degradation of castor oil and urethane linkages between 543 and 753 K, the addition of ZnO did not induce any chemical modifications in the COPs, whose ATR-FTIR peaks matched those of the typical polyurethane networks. The detailed description of the ATR-FTIR analyses of the COPs and ZnO/COPs as well as additional TGA and DTG are reported in the section S5 of the Supplementary Material.

Adsorption tests in saturated atmosphere of AcOH showed that all ZnO/COPs were able to absorb AcOH more effectively than acti-

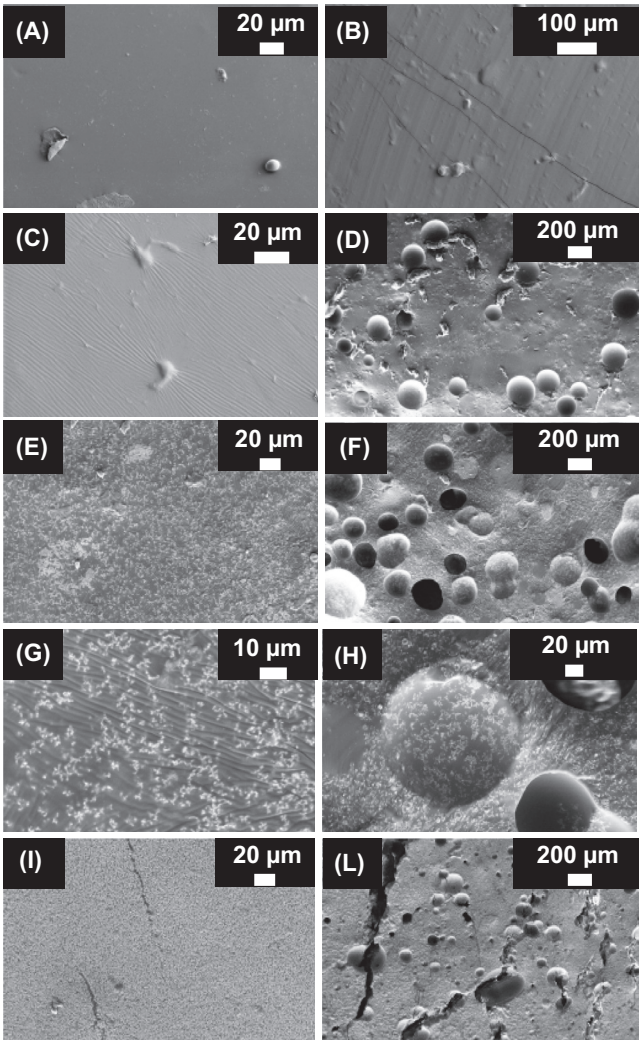

Fig. 2. SEM images of a COP (A, B), and of ZnO/COPs 10g (C, D), 30g (E, F, G, H) and 60g (I, L) composites. Images of the surfaces and sections are on the left and on the right columns, respectively. White spots correspond to ZnO particles.

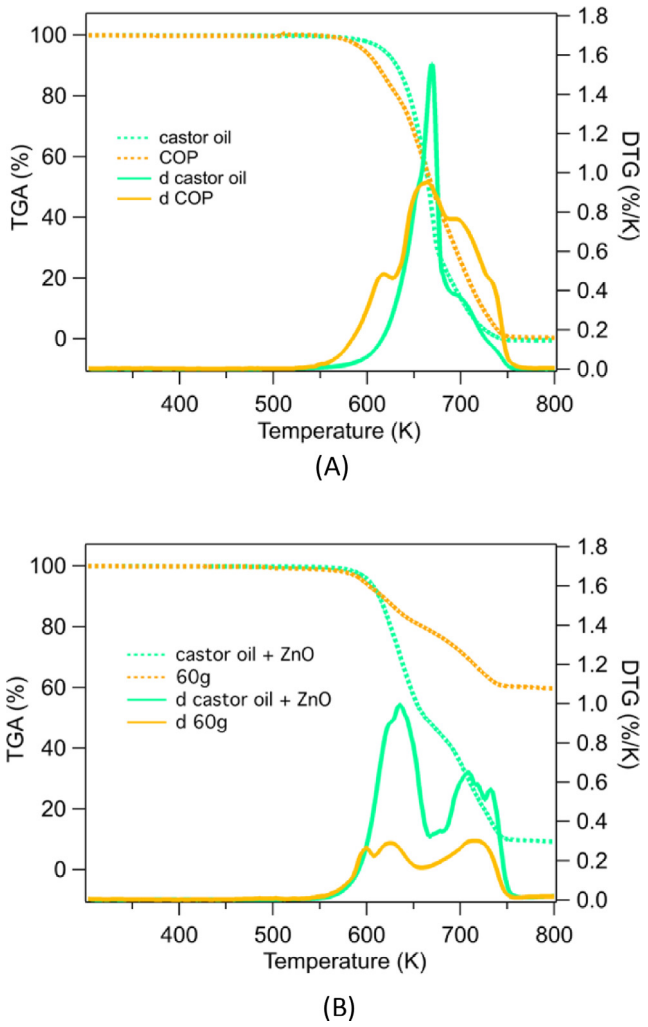

Fig. 3. TGA and DTG of: (A) castor oil and COP; (B) castor oil mixed with ZnO powder and 60g.

vated carbon, the most used adsorber for AcOH, as evidenced by Fig. 4.

The zinc oxide particles reacted with AcOH to produce zinc acetate at the particle-gas interface; the formation of the acetate was confirmed by XRD and ATR-FTIR analysis of the ZnO powders before and after adsorption tests (see section S6 in the Supplementary Material for details). Accordingly, the AcOH adsorbed increases as the surface area of the particles increases (*e.g.*, passing from ZnO-g to –e and –n).

Noticeably, also the COP had higher absorption capacity than the same mass of activated carbon benchmark, even before the addition of the ZnO particles. Its ability to remove AcOH could be explained in terms of polar interactions of the AcOH molecules with the unreacted hydroxyl groups (~85%) in the polyurethane network. This hypothesis agreed with the preliminary tests where COPs made with higher amounts of PolyHDI, *i.e.*, the resulting COP has less free hydroxyl groups, showed lower adsorption capacities (see section S2 in the Supplementary Material).

The addition of 30%$_{wt}$ or 60%$_{wt}$ ZnO to the COPs further enhanced AcOH absorption, and the increase was more evident when nano-sized particles were used. The adsorption capacities of the ZnO/COPs were compared with the balanced sum (green bars in Fig. 4) of the capacity of pure COPs and of the corresponding ZnO powder, *e.g.*, sample 30g was compared with the sum of 30% the adsorption capacity of ZnO g-powder and 70% the capacity of a COP (being composed by 30%$_{wt}$ of ZnO powder and 70%$_{wt}$ of COP). It was evident that the absorption capacities of the ZnO/COPs were almost comparable with those of powdery zinc oxide, except in the case of nano-sized particles. In this latter case the lower adsorption capacities of the ZnO/COPs "n" samples could be ascribed to partial aggregation of the particles during the preparation of the composites. However even in this case, the ZnO/COPs composites retain the advantage of being easily handled and movable, with no risk of dispersing particulate into display cases/crates or on the surface of neighboring works of art, whereas free, non-confined ZnO powders or activated charcoal can be easily dispersed in display cases/crates.

After the adsorption tests in saturated atmosphere of AcOH, all samples were placed under vacuum (15 mbar), and adsorption capacities were recalculated to evaluate the amount of chemisorbed, or at least strongly physiosorbed, AcOH.[58] Results are shown in Fig. 5.

The ZnO/COPs (30%$_{wt}$ or 60%$_{wt}$ ZnO content) retained significantly larger amounts of AcOH than the activated carbon benchmark, as the acetic acid was stably fixed into zinc acetate. Instead, AcOH retention by pure COPs was very low, indicating that the polyurethane network interacted with the acid through weak physisorption. Strikingly, the adsorption capacities of the compos-

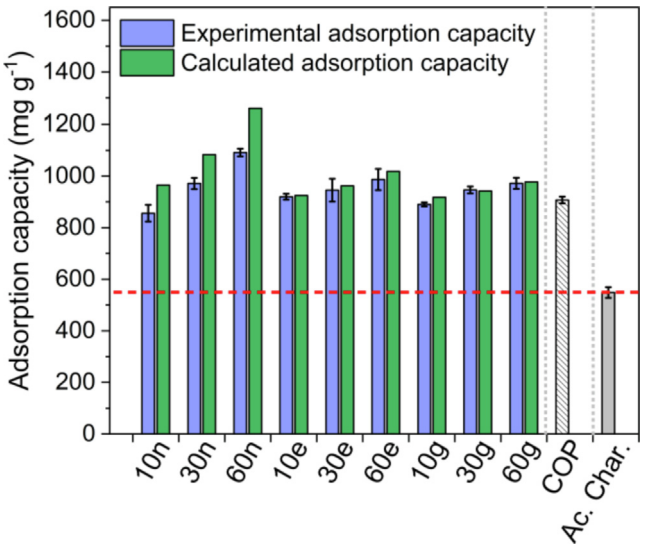

Fig. 4. Adsorption capacities of ZnO/COPs (blue bars: 10n, e, g; 30n, e, g; 60n, e, g), COP (dashed bar) and commercially available activated charcoal (gray bar, "Ac. Char.") at the equilibrium in saturated atmosphere of AcOH (after 1530 h adsorption at 293 K). Powdery "n", "g" and "e" ZnO adsorbed 1451 ± 45, 1015 ± 21 and 931 ± 28 mg of acetic acid *per* g of powder, respectively. For each ZnO/COP, the green bar shows the calculated capacity of a balanced sum of COP (70–90% contribution) and non-confined ZnO powder (10–30% contribution), for comparison with the experimentally measured capacities of the composites. (For interpretation of the references to color in this figure legend, the reader is referred to the web version of this article.)

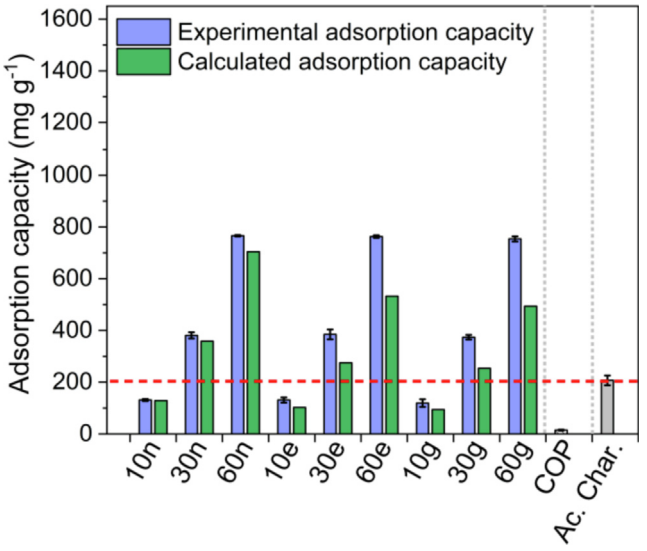

Fig. 5. Adsorption capacities of ZnO/COPs (blue bars: 10n,e,g; 30n,e,g; 60n,e,g), COP (dashed bar) and commercially available activated charcoal (gray bar, "Ac. Char.") after adsorption tests in saturated atmosphere of AcOH and 350 h desorption under vacuum (15 mbar). Powdery "n", "g" and "e" ZnO adsorbed 1164 ± 37, 880 ± 14 and 814 ± 22 mg of acetic acid *per* g of powder after adsorption tests, respectively. For each ZnO/COP, the green bar shows the calculated capacity of a balanced sum of COP (70% contribution) and non-confined ZnO powder (30% contribution), for comparison with the experimentally measured capacities of the composites. (For interpretation of the references to color in this figure legend, the reader is referred to the web version of this article.)

ites were in this case higher than those of the balanced sums of separated COPs and ZnO powders, especially for ZnO/COPs with 30%$_{wt}$ and 60%$_{w}$ ZnO content. This behavior is further highlighted considering the quantity of ZnO converted into zinc acetate (see Table S7 in the Supplementary Material), which in the ZnO/COPs was 15–20% higher than in the ZnO micropowders (ZnO-e and ZnO-g), and comparable (or slightly higher) than in the nanopowder (ZnO-n). The fact that the oxide conversion into acetate never surpasses 55% was explained considering that the formation of zinc acetate layers at the surface of the particles likely hinders further diffusion of AcOH in their inner core; thus, the higher the surface area of the particles, the higher the amount of converted ZnO.

While no morphological alteration of the COPs is observable after adsorption and desorption of AcOH (see SEM images in Fig. 6 A, B), the surface and section of ZnO/COPs samples were populated with zinc-containing 10–100 μm tetragonal pyramid microcrystals, (for additional SEM images and for TGA and DTG analysis, see sections S9 and S10 in the Supplementary Material), which were assumed to be zinc acetate. The crystals also surface out of the COP structure, likely due to the diffusion of zinc ions through the polyurethane matrix, driven by concentration gradients, when ZnO reacted with AcOH; the diffusion of the zinc ions in the COP was expected to compete with the surface passivation of the ZnO particles, favoring their conversion into acetate.

ATR-FTIR measurements (Fig. S10 in the Supplementary Material) and 2D FTIR Imaging (Fig. 7) confirmed the formation of zinc acetate in the composites. The IR spectra show peaks at 1595 and 1542 cm^{-1} (doublet), 1430 cm^{-1} and 1380 cm^{-1} corresponding,

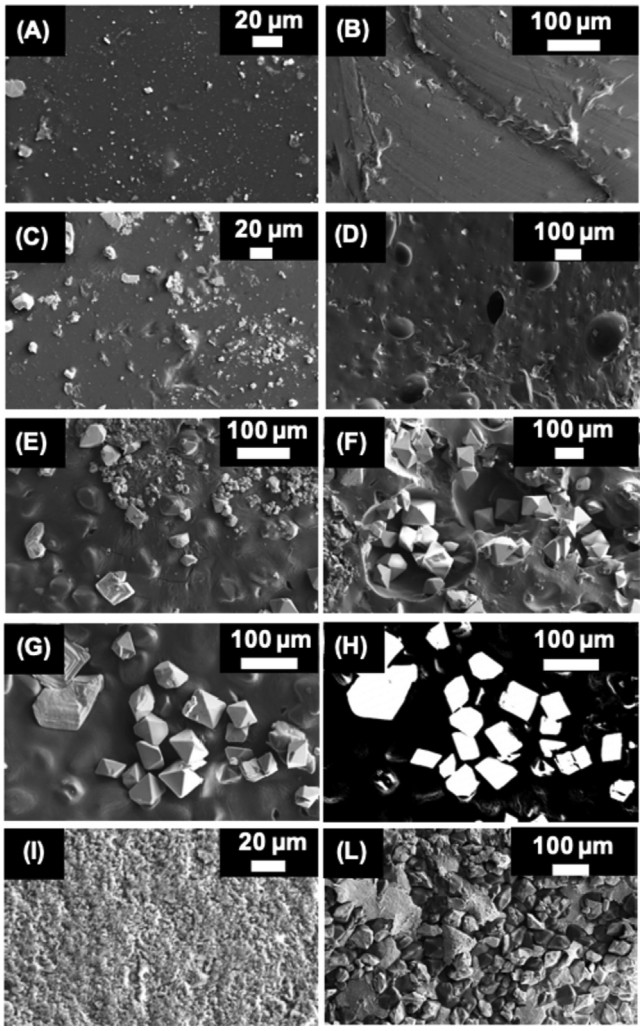

Fig. 6. SEM images of a COP (A, B), and of ZnO/COPs 10g (C, D), 30g (E, F, G and H-backscattered electrons SEM), 60g (I, L) composites. The images of the surfaces and sections of the samples (except for H) are on the left and on the right columns, respectively.

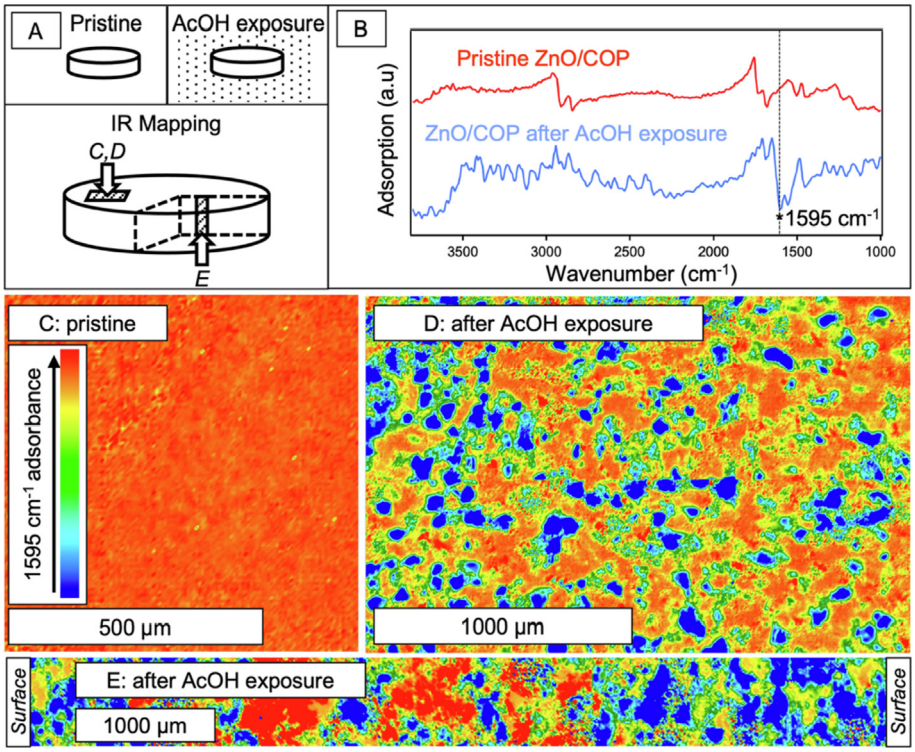

Fig. 7. (A, B, C) 2D FTIR Imaging maps showing the intensity of the zinc acetate IR band at 1595 cm^{-1} (COO^- asymmetric stretching) on the surface and across the section of a ZnO/COP after exposure to AcOH. The IR maps are related to different portions of the COP, as illustrated in panel A. The band appeared as strong derivative shaped peak in the reflectance spectra (B); each spectrum was related to a pixel (5.5 × 5.5 μm^2) of the maps. The negative part of the peak is imaged as blue-green pixels in the false color IR maps, whereas the polyurethane matrix appears as yellow–red pixels. (C) Surface map of a pristine ZnO/COP 30 g sample. (D, E) Surface and section maps of the same sample after adsorption and desorption tests in saturated atmosphere of AcOH. (For interpretation of the references to color in this figure legend, the reader is referred to the web version of this article.)

respectively, to the COO^- asymmetric and symmetric stretching vibrations and to the CH_3 symmetric bending of the salt.[59,60] The absorption at 1595 cm^{-1} appeared in the reflectance spectra as a strong derivative shaped peak (Fig. 7 B), whose negative part was imaged as blue and green pixels in the IR false color maps, so as to visualize the distribution of zinc acetate domains on the surface and through the section of the polyurethane network (red-yellow pixels background in Fig. 7 C-E). The acetate domains had dimensions consistent with those of the crystals observed with SEM, and were distributed across the entire length of the COPs section (Fig. 7 C), proving the homogeneous diffusion of AcOH through the matrix during adsorption of the VOC. The weak and largely reversible physisorption of AcOH into the polyurethane network might play an important role in promoting the transport of the acid to the surface of the ZnO particles embedded in the COPs, which could explain the higher conversion into acetate inside the composites with respect to oxide powders simply packed into a vial.

Overall, even though the ZnO/COPs with 60%$_{wt}$ ZnO showed the highest AcOH retention, these materials tend to be crumbling, owing to the high content of ZnO powder. The ZnO/COPs with 30%$_{wt}$ ZnO can be thus considered as the best performing formulations in the series, having almost twice the adsorption capacities of activated charcoal, in addition to optimal mechanical properties and compactness. In particular, ZnO/COP 30g was deemed as the ideal candidate for possible large-scale production and applications to art preventive conservation, as this composite had comparable performance to its 30e and 30n analogues while employing affordable ZnO micropowder (<44 µm), and considering some possible toxicity issues related to ZnO nanoparticles.[61] This type of ZnO/COP was thus selected for further adsorption trials, either in the 54 L glass reactors at low initial AcOH concentration, and in a real case scenario where the composites were placed in a wooden crate (where AcOH is continuously emitted [62]), such as those commonly used in the storage deposits and display cases in museums and art collections. In the first case, the ZnO/COP 30g decreased AcOH concentration from 6240 ± 15 down to 155 ± 21 ppbv (>97% reduction), *i.e.*, below the standard limit of 400 ppbv typically suggested for the preventive conservation of Cultural Heritage objects in museums and display cases.[63] Instead, a COP with no zinc oxide decreased it to 321 ± 9 ppbv. Absorption of AcOH by the ZnO/COP 30g in the wooden crate was tested over 45 days (see Fig. S11 in the Supplementary Material for details). In the first week, the composite reduced the concentration of AcOH down to<250 ppbv from an initial concentration of almost 600 ppbv and in the following weeks the concentration of acetic acid was kept constantly below the limit of 400 ppmv. Finally, the color changes of the ZnO/COP 10, 30 and 60g were monitored as the composites were being exposed to AcOH. The newly formed transparent crystals of zinc acetate replaced white ZnO, revealing the original slightly yellowish hue of the COPs. Such discoloration of the composites upon exposure to AcOH could be feasibly exploited in practical applications as an indicator to replace the adsorbers in display cases (see Fig. S11 in the Supplementary Material for a picture of the materials prior and after exposure to acetic acid).

4. Conclusions

Novel inorganic–organic composite systems for the efficient removal of acetic acid were prepared combining a polyurethane derived from castor oil with ZnO micron- or nano-sized powders, through an easy, sustainable, and up-scalable procedure.

The adsorption properties of the composites were verified operating in saturated as well as in ppbv-scale atmosphere of acetic acid, also considering the real case scenario of a wooden crate such as those typically employed in the storage deposits of museums and art collections. In saturated acetic acid atmosphere, the ZnO/COPs were proved to be more effective in the adsorption and retention of the acid (after desorption in vacuum) than commonly employed activated charcoal,[64–66] removing up to 750 mg of acetic acid *per* g of ZnO/COPs. When exposed to *ca.* 6000 ppbv of acid, the ZnO/COPs decreased the pollutant concentration of 97%, and placing the composites in a wooden crate (continuously emitting acetic acid) lowered the acid concentration below the 400 ppbv limit recommended for Cultural Heritage preservation.[63] In addition, the compact structure of ZnO/COPs prevents the dispersion of material inside display cases or crates, which could occur with non-confined powders, avoiding possible contamination of artworks or health issues.[22,63]

It was demonstrated that the adsorption capacity of the composites is due to the effective transport of acetic acid inside the COP matrix, up to reach the surface of the ZnO particles, where the acid is neutralized to zinc acetate. The surface area of the ZnO particles affected the amount of oxide converted into acetate, as expected considering that the reaction with acetic acid took place at the interface between the particles and the polyurethane. Weak interactions between the polyurethane matrix and acetic acid likely favoured the transport of the acid up to reach the surface of the oxide particles, producing a synergetic effect in the ZnO/COPs and better performances than non-confined ZnO simply packed in containers.

Further investigation of such synergic effect could act as a springboard for additional applications of the composites not limited to the removal of acetic acid but also to other types of volatile organic compounds, while future perspectives involve the study of adsorption kinetics and case-study applications of the novel composites in museums, art galleries and whenever the adsorption of volatile organic compounds is requested.

CRediT authorship contribution statement

Alessio Zuliani: Conceptualization, Data curation, Formal analysis, Investigation, Methodology, Writing. **Damiano Bandelli:** Data curation, Formal analysis, Investigation, Methodology, Writing. **David Chelazzi:** Conceptualization, Data curation, Formal analysis, Methodology, Writing. **Rodorico Giorgi:** Conceptualization, Data curation, Formal analysis, Methodology, Writing. **Piero Baglioni:** Supervision, Conceptualization, Validation, Data curation, Formal analysis, Funding acquisition, Methodology, Project administration, Writing.

Declaration of Competing Interest

The authors declare that they have no known competing financial interests or personal relationships that could have appeared to influence the work reported in this paper.

Acknowledgements

This project has received funding from the European Union's Horizon 2020 research and innovation programme under grant agreement No814496. CSGI is also acknowledged for partially funding this work.

Appendix A. Supplementary material

Supplementary data to this article can be found online at https://doi.org/10.1016/j.jcis.2022.01.123.

References

[1] L. Nie, B. Duan, A. Lu, L.N. Zhang, Pd/TiO_2 @ Carbon Microspheres Derived from Chitin for Highly Efficient Photocatalytic Degradation of Volatile Organic Compounds, ACS Sustainable Chem. Eng. 7 (1) (2019) 1658–1666.
[2] A. Schieweck, B. Lohrengel, N. Siwinski, C. Genning, T. Salthammer, Organic and inorganic pollutants in storage rooms of the Lower Saxony State Museum Hanover, Germany, Atmospheric Environment 39 (33) (2005) 6098–6108.
[3] M. Smielowska, M. Marc, B. Zabiegala, Indoor air quality in public utility environments-a review, Environ. Sci. Pollut. Res. 24 (12) (2017) 11166–11176.
[4] D. Chelazzi, A. Chevalier, G. Pizzorusso, R. Giorgi, M. Menu, P. Baglioni, Characterization and degradation of poly(vinyl acetate)-based adhesives for canvas paintings, Polym. Degrad. Stab. 107 (2014) 314–320.
[5] L.T. Gibson, B.G. Cooksey, D. Littlejohn, N.H. Tennent, A diffusion tube sampler for the determination of acetic acid and formic acid vapours in museum cabinets, Anal. Chim. Acta 341 (1) (1997) 11–19.
[6] T. Oikawa, T. Matsui, Y. Matsuda, T. Takayama, H. Niinuma, Y. Nishida, K. Hoshi, M. Yatagai, Volatile organic compounds from wood and their influences on museum artifact materials I. Differences in wood species and analyses of causal substances of deterioration, Journal of Wood Science 51 (4) (2005) 363–369.
[7] N. De Laet, S. Lycke, J. Van Pevenage, L. Moens, P. Vandenabeele, Investigation of pigment degradation due to acetic acid vapours: Raman spectroscopic analysis, Eur. J. Mineral. 25 (5) (2013) 855–862.
[8] J. La Nasa, I. Degano, F. Modugno, M.P. Colombini, Effects of acetic acid vapour on the ageing of alkyd paint layers: Multi-analytical approach for the evaluation of the degradation processes, Polym. Degrad. Stab. 105 (2014) 257–264.
[9] M. Malagodi, M. Licchelli, S. Bottigliero, C. Milanese, P. Cofrancesco, T. Rovetta, Ieee, Alteration processes of pigments exposed to acetic and formic acid vapors, 2017 1st Ieee International Conference on Environment and Electrical Engineering and 2017 17th Ieee Industrial and Commercial Power Systems Europe (Eeeic / I&Cps Europe) (2017).
[10] X.Q. Li, L. Zhang, Z.Q. Yang, P. Wang, Y.F. Yan, J.Y. Ran, Adsorption materials for volatile organic compounds (VOCs) and the key factors for VOCs adsorption process: A review, Sep. Purif. Technol. 235 (2020).
[11] J.W. Ren, X. Dyosiba, N.M. Musyoka, H.W. Langmi, M. Mathe, S.J. Liao, Review on the current practices and efforts towards pilot-scale production of metal-organic frameworks (MOFs), Coord. Chem. Rev. 352 (2017) 187–219.
[12] A.R. Martins, I.T. Cunha, A.A.S. Oliveira, F.C.C. Moura, Highly ordered spherical SBA-15 catalysts for the removal of contaminants from the oil industry, Chem. Eng. J. 318 (2017) 189–196.
[13] F. Ferlin, T. Giannoni, A. Zuliani, O. Piermatti, R. Luque, L. Vaccaro, Sustainable Protocol for the Reduction of Nitroarenes by Heterogeneous Au@SBA-15 with $NaBH_4$ under Flow Conditions, ChemSusChem 12 (13) (2019) 3178–3184.
[14] A. Zuliani, P. Ranjan, R. Luque, E.V. Van der Eycken, Heterogeneously Catalyzed Synthesis of Imidazolones via Cycloisomerizations of Propargylic Ureas Using Ag and Au/Al SBA-15 Systems, ACS Sustainable Chem. Eng. 7 (5) (2019) 5568–5575.
[15] S.B. Wang, Y.L. Peng, Natural zeolites as effective adsorbents in water and wastewater treatment, Chem. Eng. J. 156 (1) (2010) 11–24.
[16] M. Ghidotti, D. Fabbri, A. Hornung, Profiles of Volatile Organic Compounds in Biochar: Insights into Process Conditions and Quality Assessment, ACS Sustainable Chem. Eng. 5 (1) (2017) 510–517.
[17] O. Hwang, S.R. Lee, S. Cho, K.S. Ro, M. Spiehs, B. Woodbury, P.J. Silva, D.W. Han, H. Choi, K.Y. Kim, M.W. Jung, Efficacy of Different Biochars in Removing Odorous Volatile Organic Compounds (VOCs) Emitted from Swine Manure, ACS Sustainable Chem. Eng. 6 (11) (2018) 14239–14247.
[18] A. Zuliani, M. Cano, F. Calsolaro, A.R. Puente Santiago, J.J. Giner-Casares, E. Rodríguez-Castellón, G. Berlier, G. Cravotto, K. Martina, R. Luque, Improving the electrocatalytic performance of sustainable Co/carbon materials for the oxygen evolution reaction by ultrasound and microwave assisted synthesis, Sustainable, Energy Fuels 5 (3) (2021) 720–731.
[19] Q.L. Qian, S.Y. Shao, F. Yan, G.Q. Yuan, Direct removal of trace ionic iodide from acetic acid via porous carbon spheres, J. Colloid Interface Sci. 328 (2) (2008) 257–262.
[20] X.Y. Zhao, X. Li, T.L. Zhu, X.L. Tang, Adsorption behavior of chloroform, carbon disulfide, and acetone on coconut shell-derived carbon: experimental investigation, simulation, and model study, Environ. Sci. Pollut. Res. 25 (31) (2018) 31219–31229.
[21] G.X. Zhang, Y.Y. Liu, S.L. Zheng, Z. Hashisho, Adsorption of volatile organic compounds onto natural porous minerals, J. Hazard. Mater. 364 (2019) 317–324.
[22] T.C. Arnold, B.H. Willis, F. Xiao, S.A. Conrad, D.L. Carden, Aspiration of activated charcoal elicits an increase in lung microvascular permeability, J. Toxicology-Clinical Toxicol. 37 (1) (1999) 9–16.
[23] L.P. Sycheva, R.I. Mikhailova, N.N. Belyaeva, V.S. Zhurkov, V.V. Yurchenko, O.N. Savostikova, A.V. Alekseeva, E.K. Krivtsova, M.A. Kovalenko, L.V. Ahaltseva, S. M. Sheremet'eva, N.A. Yurtseva, L.V. Muravyeva, Study of Mutagenic and

Cytotoxic Effects of Multiwalled Carbon Nanotubes and Activated Carbon in Six Organs of Mice In Vivo, Nanotechnol. Russ. 10 (3–4) (2015) 311–317.
[24] J. Pires, A.C. Araujo, A.P. Carvalho, M.L. Pinto, J.M. Gonzalez-Calbet, J. Ramirez-Castellanos, Porous materials from clays by the gallery template approach: synthesis, characterization and adsorption properties, Microporous Mesoporous Mater. 73 (3) (2004) 175–180.
[25] X.Y. Zhang, B. Gao, A.E. Creamer, C.C. Cao, Y.C. Li, Adsorption of VOCs onto engineered carbon materials: A review, J. Hazard. Mater. 338 (2017) 102–123.
[26] H.A. Nash, The European Commission's sustainable consumption and production and sustainable industrial policy action plan, J. Cleaner Prod. 17 (4) (2009) 496–498.
[27] S.S. Wang, L. Zhang, C. Long, A.M. Li, Enhanced adsorption and desorption of VOCs vapor on novel micro-mesoporous polymeric adsorbents, J. Colloid Interface Sci. 428 (2014) 185–190.
[28] C. Kroll, A. Warchold, P. Pradhan, Sustainable Development Goals (SDGs): Are we successful in turning trade-offs into synergies?, Palgrave Communications 5 (2019)
[29] C.M. Cova, A. Zuliani, R. Manno, V. Sebastian, R. Luque, Scrap waste automotive converters as efficient catalysts for the continuous-flow hydrogenations of biomass derived chemicals, Green Chem. 22 (4) (2020) 1414–1423.
[30] P. Kynclova, S. Upadhyaya, T. Nice, Composite index as a measure on achieving Sustainable Development Goal 9 (SDG-9) industry-related targets: The SDG-9 index, Appl. Energy 265 (2020).
[31] A. Zuliani, C.M. Cova, R. Manno, V. Sebastian, A.A. Romero, R. Luque, Continuous flow synthesis of menthol via tandem cyclisation-hydrogenation of citronellal catalysed by scrap catalytic converters, Green Chem. 22 (2) (2020) 379–387.
[32] T. Mallat, A. Baiker, Potential of Gold Nanoparticles for Oxidation in Fine Chemical Synthesis, in: J.M. Prausnitz (Ed.), Annual Review of Chemical and Biomolecular Engineering, Vol 32012, pp. 11-28.
[33] Y.H. Wei, B.Y. Wang, Y. Zhang, M. Zhang, Q. Wang, H. Wu, Rational Design of Multifunctional Integrated Host Configuration with Lithiophilicity-Sulfiphilicity toward High-Performance Li-S Full Batteries, Adv. Funct. Mater. 31 (3) (2021).
[34] Y.T. Yan, P.C. Wang, J.H. Lin, J. Cao, J.L. Qi, Modification strategies on transition metal-based electrocatalysts for efficient water splitting, Journal of Energy, Chemistry 58 (2021) 446–462.
[35] F.P. Susana, J. Franco, María, I. Martinez Garcia, Raghunanan, L. Cindy, G. Frankenbach, Marie, EP3453729A1 - Adhesives derived from castor oil, EP3453729A1 - Adhesives derived from castor oil, Procter and Gamble International Operations SA, EP3453729A1 - Adhesives derived from castor oil, 2018.
[36] H.D. Santan, C. James, E. Fratini, I. Martinez, C. Valencia, M.C. Sanchez, J.M. Franco, Structure-property relationships in solvent free adhesives derived from castor oil, Ind. Crops Prod. 121 (2018) 90–98.
[37] A.M. Borrero-Lopez, D.B. Guzman, J.A. Gonzalez-Delgado, J.F. Arteaga, C. Valencia, U. Pischel, J.M. Franco, Toward UV-Triggered Curing of Solvent-Free Polyurethane Adhesives Based on Castor Oil, ACS Sustainable Chem. Eng. 9 (33) (2021) 11032–11040.
[38] R. Meininghaus, S. Kirchner, F. Maupetit, H. Sallee, D. Quenard, Gravimetric studies on VOC adsorption by indoor materials under near-ambient conditions, Indoor Built Environ. 9 (5) (2000) 277–283.
[39] L. Li, S.Q. Liu, J.X. Liu, Surface modification of coconut shell based activated carbon for the improvement of hydrophobic VOC removal, J. Hazard. Mater. 192 (2) (2011) 683–690.
[40] I. Krasevec, E. Menart, M. Strlic, I.K. Cigic, Validation of passive samplers for monitoring of acetic and formic acid in museum environments, Heritage Science 9 (1) (2021).
[41] L.T. Gibson, C.M. Watt, Acetic and formic acids emitted from wood samples and their effect on selected materials in museum environments, Corros. Sci. 52 (1) (2010) 172–178.
[42] M. Ghasemlou, F. Daver, E.P. Ivanova, B. Adhikari, Polyurethanes from seed oil-based polyols: A review of synthesis, mechanical and thermal properties, Ind. Crops Prod. 142 (2019).
[43] I. Chakraborty, K. Chatterjee, Polymers and Composites Derived from Castor Oil as Sustainable Materials and Degradable Biomaterials: Current Status and Emerging Trends, Biomacromolecules 21 (12) (2020) 4639–4662.
[44] F.V. Amorim, R.J.R. Padilha, G.M. Vinhas, M.R. Luiz, N.C. de Souza, Y.M.B. de Almeida, Development of hydrophobic polyurethane/castor oil biocomposites with agroindustrial residues for sorption of oils and organic solvents, J. Colloid Interface Sci. 581 (2021) 442–454.
[45] J.Y. Lu, Y. Zhang, Y.J. Tao, B.B. Wang, W.H. Cheng, G.X. Jie, L. Song, Y. Hu, Self-healable castor oil-based waterborne polyurethane/MXene film with outstanding electromagnetic interference shielding effectiveness and excellent shape memory performance, J. Colloid Interface Sci. 588 (2021) 164–174.
[46] L. Zhou, T. Li, W.K. Zhang, Vibrational relaxation dynamics of a potential local infrared probe: Isocyanate, Chem. Phys. 536 (2020).
[47] D.J.C. Constable, A.D. Curzons, V.L. Cunningham, Metrics to 'green' chemistry - which are the best?, Green Chem 4 (6) (2002) 521–527.
[48] R.A. Sheldon, The E factor 25 years on: the rise of green chemistry and sustainability, Green Chem. 19 (1) (2017) 18–43.
[49] C. Maria Cova, A. Zuliani, M.J. Munoz-Batista, R. Luque, Efficient Ru-based scrap waste automotive converter catalysts for the continuous-flow selective hydrogenation of cinnamaldehyde, Green Chem. 21 (17) (2019) 4712–4722.
[50] M. Tobiszewski, M. Marc, A. Galuszka, J. Namiesnik, Green Chemistry Metrics with Special Reference to Green Analytical Chemistry, Molecules 20 (6) (2015) 10928–10946.
[51] L. Pari, A. Suardi, W. Stefanoni, F. Latterini, N. Palmieri, Environmental and Economic Assessment of Castor Oil Supply Chain: A Case Study, Sustainability 12 (16) (2020).
[52] H. Sardon, D. Mecerreyes, A. Basterretxea, L. Averous, C. Jehanno, From Lab to Market: Current Strategies for the Production of Biobased Polyols, ACS Sustainable Chem. Eng. 9 (32) (2021) 10664–10677.
[53] T.E. Graedel, R.J. Klee, Getting serious about sustainability, Environ. Sci. Technol. 36 (4) (2002) 523–529.
[54] K.S. Ng, I. Head, G.C. Premier, K. Scott, E. Yu, J. Lloyd, J. Sadhukhan, A multilevel sustainability analysis of zinc recovery from wastes, Resour. Conserv. Recycl. 113 (2016) 88–105.
[55] C.M. Cova, A. Zuliani, M.J. Munoz-Batista, R. Luque, A Sustainable Approach for the Synthesis of Catalytically Active Peroxidase-Mimic ZnS Catalysts, ACS Sustainable Chem. Eng. 7 (1) (2019) 1300–1307.
[56] M.M. Conceicao, R.A. Candeia, F.C. Silva, A.F. Bezerra, V.J. Fernandes, A.G. Souza, Thermo analytical characterization of castor oil biodiesel, Renew. Sustain. Energy Rev. 11 (5) (2007) 964–975.
[57] V.B. Borugadda, V.V. Goud, Comparative studies of thermal, oxidative and low temperature properties of waste cooking oil and castor oil, J. Renewable Sustainable Energy 5 (6) (2013).
[58] X. Zhou, W.Y. Huang, J. Shi, Z.X. Zhao, Q.B. Xia, Y.W. Li, H.H. Wang, Z. Li, A novel MOF/graphene oxide composite GrO@MIL-101 with high adsorption capacity for acetone, J. Mater. Chem. A 2 (13) (2014) 4722–4730.
[59] Y.Q. Lu, J.D. Miller, Carboxyl stretching vibrations of spontaneously adsorbed and LB-transferred calcium carboxylates as determined by FTIR internal reflection spectroscopy, J. Colloid Interface Sci. 256 (1) (2002) 41–52.
[60] H. Yin, P.S. Casey, ZnO nanorod composite with quenched photoactivity for UV protection application, Mater. Lett. 121 (2014) 8–11.
[61] N. Hadrup, F. Rahmani, N.R. Jacobsen, A.T. Saber, P. Jackson, S. Bengtson, A. Williams, H. Wallin, S. Halappanavar, U. Vogel, Acute phase response and inflammation following pulmonary exposure to low doses of zinc oxide nanoparticles in mice, Nanotoxicology 13 (9) (2019) 1275–1292.
[62] S. Msallamova, M. Kouril, K.C. Strachotova, J. Stoulil, K. Popova, P. Dvorakova, M. Lhotka, Protection of lead in an environment containing acetic acid vapour by using adsorbents and their characterization, Heritage Science 7 (1) (2019).
[63] J. Tétreault, Control of Pollutants in Museums and Archives – Technical Bulletin 37, in: D.o.C. Heritage (Ed.) Government of Canada, Canadian Conservation Institute, Canada, 2021.
[64] M.J. Ruhl, Recover Vocs Via Adsorption On Activated Carbon, Chem. Eng. Prog. 89 (7) (1993) 37–41.
[65] C.L. Chuang, P.C. Chiang, E.E. Chang, Modeling VOCs adsorption onto activated carbon, Chemosphere 53 (1) (2003) 17–27.
[66] B. Cardoso, A.S. Mestre, A.P. Carvalho, J. Pires, Activated carbon derived from cork powder waste by KOH activation: Preparation, characterization, and VOCs adsorption, Ind. Eng. Chem. Res. 47 (16) (2008) 5841–5846.